JOURNAL OF MATERIALS SCIENCE 18 (1983) 1202–1212

A three-dimensional approach to the electrolytic degradation of solid electrolytes

ANIL V. VIRKAR, L. VISWANATHAN
Department of Materials Science and Engineering, University of Utah, Salt Lake City, Utah 84112, USA

A semiquantitative three-dimensional analysis of the electrolytic degradation of solid electrolytes is presented. This analysis leads to critical current densities that are in accord with experimental observations in contrast with the two-dimensional models which lead to a discrepancy of three orders of magnitude. The effect of microstructure has also been incorporated into the analysis.

1. Introduction

It is well known that under certain conditions solid electrolytes are subject to a type of degradation which manifests itself in the form of thin metallic filaments originating from the ion-neutralization surface. While this type of degradation can occur in all cationic conductors, it has been studied extensively in sodium β- and β''-aluminas due to their use as sodium ion conductor membranes in the sodium–sulphur battery. Specifically, it has been found that under the conditions of charging, sodium filaments often originate at the liquid sodium–β''-alumina interface and propagate through the thickness of the solid electrolyte eventually leading to the shorting of the battery. Experimental observations [1] indicate that the sodium filaments are in the form of thin ribbons.

Several researchers have attempted to model the process of degradation. Armstrong *et al.* [1] proposed that sodium ions in the vicinity of a sodium filled surface crack are attracted towards the crack. Sodium ions are neutralized at the metal/solid electrolyte interface and the sodium metal formed flows towards the open end. The essence of the model given by Armstrong *et al.* [1] lies in the premise that when the pressure generated exceeds the critical pressure so that the Griffith equation is satisfied, degradation ensues.

Concurrently, Richman *et al.* [2, 3] presented a model wherein the process of degradation was presumed to occur by a stress corrosion mechanism. In the approaches by Armstrong *et al.* [1] and Richman *et al.* [2] it was assumed that the crack had a fixed (arbitrarily) thickness and that the equations of two-dimensional fracture mechanics were applicable. However, the assumption of constant thickness is incorrect within the formalism of the theory of linear elasticity. Subsequently, Shetty *et al.* [4] removed the restriction of fixed crack thickness. Using the method of Sneddon and Das [5], they determined the shape of the crack under the conditions of fluid flow. As a first iteration, Shetty *et al.* [4] assumed the crack to consist of a flat parallel sided channel (thickness of which is determined self-consistently). For a rectangular channel of constant cross-section, the pressure head varies linearly with length. Therefore, assuming a linearly varying loading on the surface of the crack, Shetty *et al.* [4] determined the shape of the crack which turned out to be nearly flat and parallel up to about $0.8l$ where l is the crack length. Thus, the loading generated by the fluid flow and the resultant crack shape were shown to be compatible to a first approximation. (Recently, Feldman and DeJonghe [6] have attempted to solve this problem. However, in their analysis they assumed the crack to be of elliptical shape and for this shape they determined the pressure distribution, which is not linear but varies as $\tanh^{-1}(x/l)$. Although Feldman and DeJonghe [6] claim this to be a more accurate calculation, they have failed to recognize the fact that the crack shape is not elliptical under a pressure distribution $P(x) = P_0 \tanh^{-1}(x/l)$. Thus, the problem solved by these authors is not self-

0022–2461/83 $03.00 + .12

consistent and in fact the analysis given by Shetty *et al.* [4] is a higher order approximation.) The analysis by Shetty *et al.* [4] leads to a relation for critical current density in a natural way. For a typical flaw of length 100 μm, the critical current density was of the order of $10^4\,A\,cm^{-2}$ (there is a numerical error in the calculations given in reference [4]).

In a subsequent paper by Virkar [7], the ion focusing was incorporated by solving the Laplace equation for the appropriate boundary conditions. The critical current density, i_{cr}, for a typical flaw about 100 μm in length was once again about $10^4\,A\,cm^{-2}$ at 300° C. This demonstrated that the exact solution to the Laplace equation made a minor difference in the calculated value of the critical current density i_{cr}.

In all of the analyses on degradation of β''-alumina, the crack geometry is assumed to be two-dimensional despite the fact that the filaments grow in the form of thin ribbons [1]. The primary reason for analysing the problem using a two-dimensional linear elastic fracture mechanical framework is the resulting simplicity. An exact solution to even the two-dimensional problem where the pressure generated is due to the hydrodynamic effects is extremely complicated for the reasons enumerated in reference [4]. The three-dimensional problem is very complex if one is to attempt an exact analysis. The primary objective of this paper is to present a simplistic but a three-dimensional analysis. Through the analysis presented here which takes into account the physical processes occurring at the crack tip, critical current densities above which degradation occurs are found to be two or three orders of magnitude smaller than heretofore calculated. While an exact calculation of i_{cr} is not possible due to several complexities, the present analysis demonstrates that the degradation by the Poiseuille model is by far the primary mechanism of electrolyte failure.

Another objective of the present paper is to include the effect of microstructure and the wetting characteristics of liquid sodium on β''-alumina on the process of degradation.

2. Theoretical

2.1. Crack geometry

Experimental observations [1] (and the present work) show that sodium filaments which form at the liquid sodium–β''-alumina interface resemble thin ribbons. Our objective is to examine the conditions under which these filaments grow. The problem is clearly three-dimensional and an exact analysis is extremely complicated. However, our primary objective is to obtain an estimate of the critical current density above which degradation occurs. A great simplification can be achieved based on Saint Venant's principle [8]. Before considering the actual degradation problem, let us examine the justification for simplifications we shall make in the analysis.

Fig. 1a shows a linear elastic body containing a ribbon shaped crack of width $2c$ and length l lying in the x–y plane (the length l is along the y-axis) with loading (uniform stress σ) in the z-direction. The length of the crack, l, is smaller than the thickness of the plate, T. The geometry of the crack tip in the x–y plane is assumed to be circular with radius c. The geometry of the crack shown in Fig. 1a closely resembles the actual filaments observed.

Fig. 1b shows a plate identical to that in Fig. 1a with the exception that the crack extends through the thickness. This problem represents the usual two-dimensional plane strain problem. Finally, Fig. 1c shows a plate identical to those in Figs. 1a and b but without any crack. In the following we will assume that l is greater than $2c$.

Consider point A close to the edge of the crack as shown in Fig. 1a. The point A′ in Fig. 1b is similarly located. As long as point A is far away from the tip of the crack (M), the state of stress at points A and A′ will be nearly identical. This follows from Saint Venant's principle which postulates that the state of stress and strain at a point due to tractions applied at remote places depends only on the cumulative magnitude of the load and not on the details of the distribution. Thus, whether the crack extends through the plate or only part way through the plate is almost irrelevant as far as point A is concerned. Therefore, the state of stress as well as the crack opening displacement in the z-direction for the plate shown in Fig. 1a is essentially identical to that of the problem shown in Fig. 1b except for regions near the tip and beyond. Similarly for a point such as B in Fig. 1a, which is far from the crack, the state of stress (and strain) will be essentially identical to that for point B′ in Fig. 1c.

If the externally applied stress reaches a critical value (Fig. 1b), the crack would extend in the x–y plane along the x-direction. Similarly, for

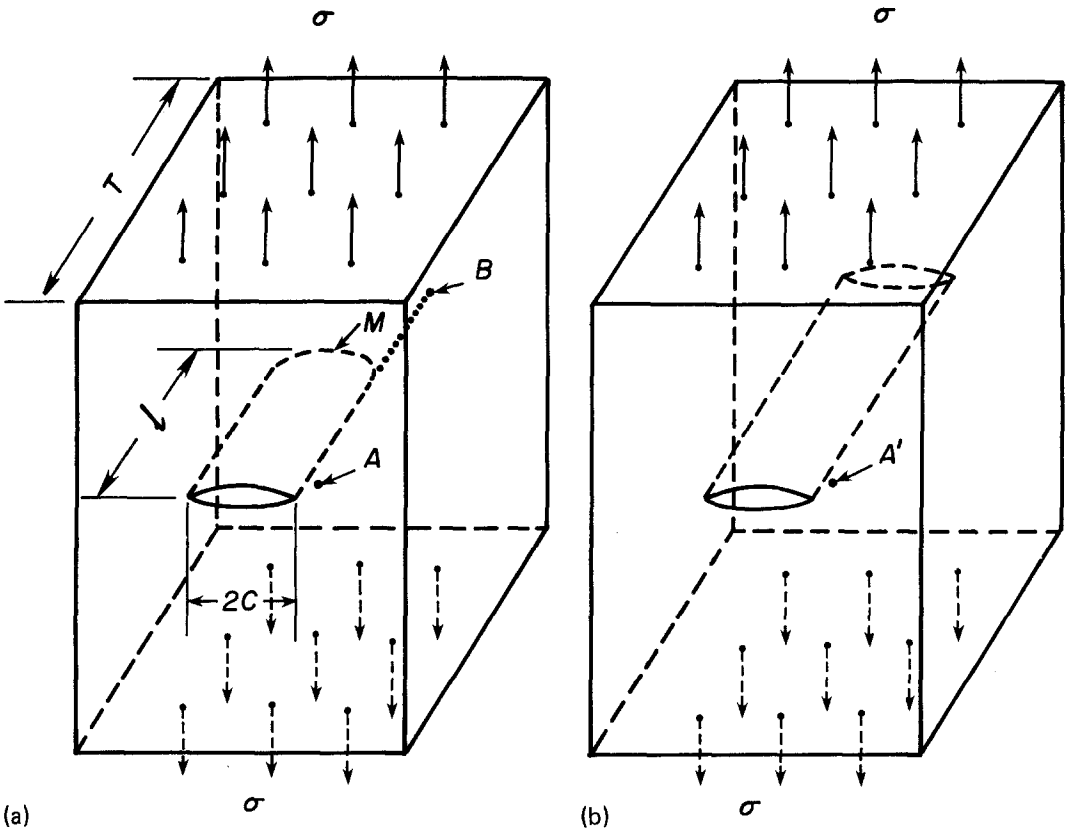

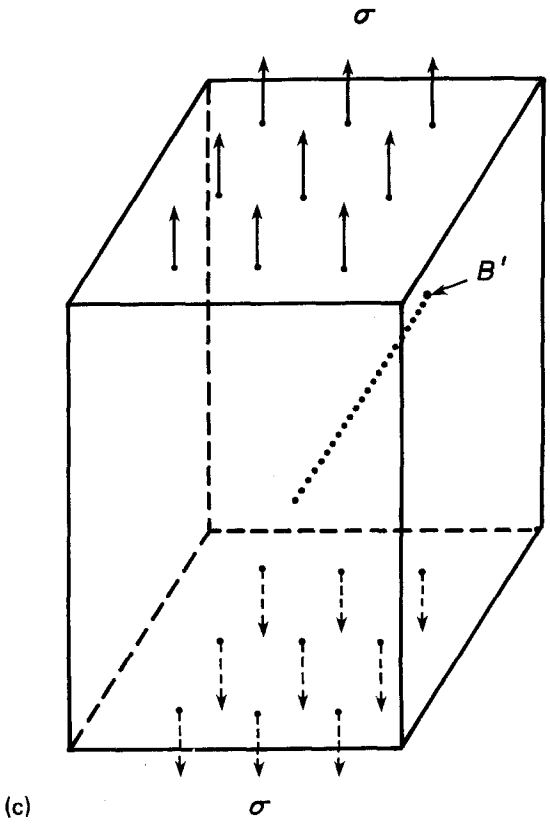

Figure 1 (a) A schematic showing a crack of length l and width $2c$ in an elastic body of thickness T ($T > l$) under a uniform tension σ. (b) A schematic showing a similar elastic body as in (a) with a crack through the thickness. (c) An elastic body without a crack. According to Saint Venant's principle, the state of stress at A and A′ as well as at B and B′ will be similar.

the plate shown in Fig. 1a, the crack would extend in the x-direction and not in the y-direction [9, 10]. Thus, the dimension of the crack that determines crack extension stress is $2c$ and not l. This is an extremely important consideration in that the length of the crack in the problem shown in Fig. 1a is immaterial with reference to failure: it is the width of the crack, $2c$, that determines the strength.

Fig. 2 represents a schematic of a two-dimensional crack as assumed in the previous models. The crack goes all the way through the width. In such a case, the length l determines the strength of the body. It is not difficult to see that such a model does not represent the actual crack in a solid electrolyte. It was adopted in previous works for the resulting analytical simplicity.

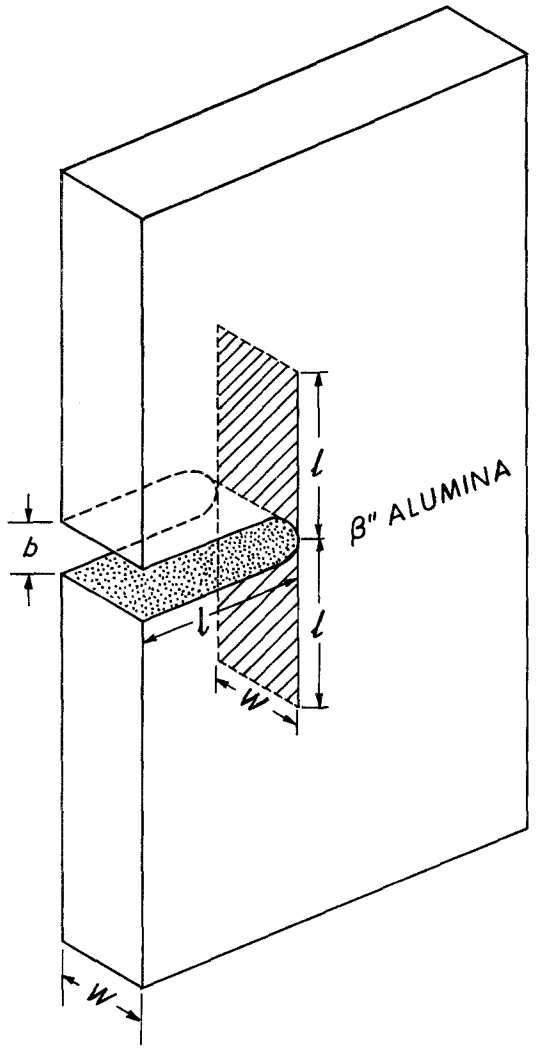

Figure 2 A schematic of the two-dimensional crack assumed in previous models along with the current focusing area, $2lw$.

2.2. Critical current density

A schematic of the crack or filament is shown in Fig. 3 with the y-axis oriented along the crack length l. For the two-dimensional problem, the flux to a sodium filled crack was determined by Virkar [7] by solving the Laplace equation. A similar calculation was subsequently repeated by Feldman and DeJonghe [6]. These calculations provide only a marginal improvement over the approximation forwarded by Richman and Tennenhouse [2] who assumed that a sodium ion that is at a distance less than l from the tip will be attracted to the tip. In the following we will make a similar assumption. Thus, it will be assumed that sodium ions in the circular region of area πl^2 (see Fig. 3) will be attracted towards the crack tip. With i as the average applied current density, the current entering the crack is

$$I(l) = i\pi l^2 \tag{1}$$

and the volume rate of sodium metal will be given by

$$\dot{V} = \frac{I(l)V_m}{F} = \frac{i\pi l^2 V_m}{F} \tag{2}$$

where V_m is the molar volume of sodium and F is the Faraday constant. (In the previous models which assume a two-dimensional crack, the sodium ions from the region $2lw$ (Fig. 2) are attracted to the tip of the crack. Assuming the width w to be unity the volume flow rate of sodium will be $(2ilV_m/F)$.)

Sodium metal will flow towards the open end and the corresponding pressure head between the tip and the open end, P_0, will be determined by the Hagen–Poiseuille law. The local pressure and the corresponding crack opening displacement are interdependent. For regions not too close to the tip of the crack, the cross-section of the crack (in the x–z plane) will be elliptical with semi-minor diameter, b, given by [11]

$$b = \frac{(1-\nu^2)cP}{E} \tag{3}$$

where P is the local pressure, E is the Young's modulus of elasticity of β''-alumina and ν is the Poisson's ratio. The area of the elliptical cross-section is πbc. For a channel of elliptical cross-section, the Hagen–Poiseuille law is given by [12]

$$\dot{V} = \left(\frac{\pi P}{4\eta l}\right)\left(\frac{c^3b^3}{(c^2+b^2)}\right) \tag{4}$$

where $\dot{V}$ is the volume flow rate, l is the length of the channel, and η is the viscosity. Now $c \gg b$, therefore,

$$\dot{V} = \frac{\pi P c b^3}{4\eta l} \tag{5}$$

(In the corresponding two-dimensional models, the Poiseuille relationship is $\dot{V} = 2b^3P/3\eta l$.) The pressure drop dP, between y and $y - dy$ is

$$dP = \frac{4\eta\dot{V}}{\pi c b^3}\,dy$$

or

$$dP = \frac{\eta V_m E^3 i l^2}{2(1-\nu^2)^3 F c^4 P^3}\,dy \tag{6}$$

where η is the viscosity of sodium. Integrating Equation 6

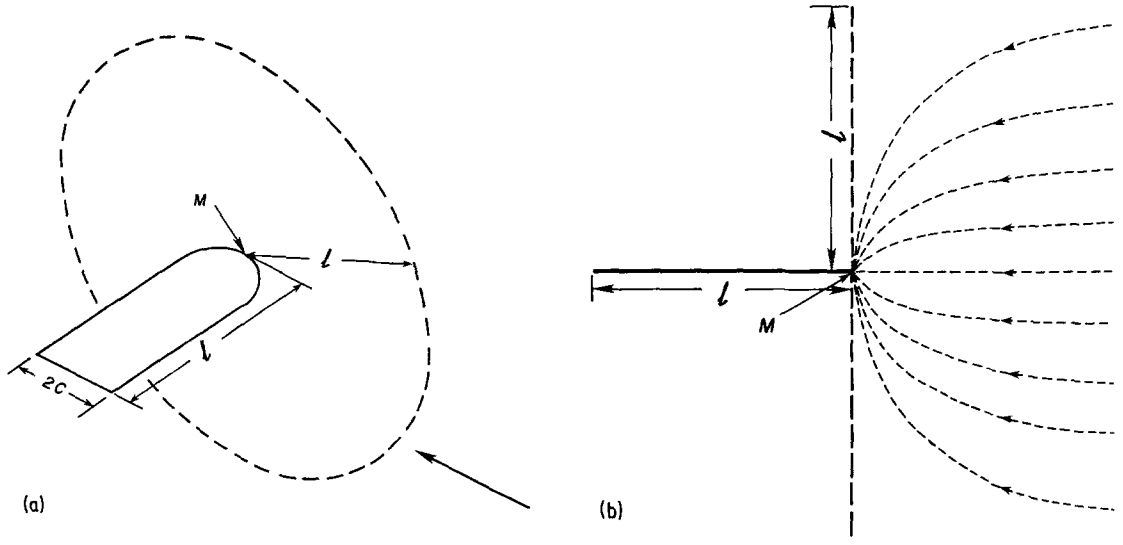

Figure 3 (a) A schematic showing a surface crack of length l and width $2c$ in a solid electrolyte. The dashed circle shows the region from which the current is focused to the crack. (b) Same as in (a) viewed along the arrow. Dashed lines indicate assumed flux lines.

$$P^4(y) = \left(\frac{2\eta V_m E^3}{(1-\nu^2)^3 F}\right)\left(\frac{l^2 i}{c^4}\right) y \qquad (7)$$

and thus $P(y) \propto y^{1/4}$ for a given crack length. For $y = l$, the maximum pressure which occurs at the tip is given by

$$P_0 = \left(\frac{2\eta V_m E^3 l^3}{(1-\nu^2)^3 F c^4}\right)^{1/4} (i)^{1/4} \qquad (8)$$

Thus the pressure at the crack tip is proportional to $l^{3/4}$ in contrast with the two-dimensional model where P_0 is found to be proportional to $l^{-1/4}$ [4, 7]. For the crack geometry shown in Fig. 3, if the loading is uniform, the crack would extend in the x-direction. However, the pressure is not uniform and is in fact highest at the crack tip. It is thus reasonable to assume that the crack will extend in the y-direction, which is consistent with the experimental observation. The crack tip is assumed to be semicircular. The criterion for crack extension should depend upon the radius c and should be independent of l. The maximum pressure must occur at point M (Fig. 1a, Fig. 2). Furthermore, the magnitude of the pressure at M (in liquid sodium) must actually be greater than P_0 since the cross-sectional area near M (in the x–z plane) will be smaller than πbc. Due to the unavailability of the actual magnitude of pressure near M it will be assumed to be P_0 in the following. This will tend to overestimate i_{cr}. The crack will extend provided the local pressure, P_0, is greater than some critical pressure, P_{cr}, which depends upon c via the Griffith relation, i.e.

$$P_{cr} \propto \frac{1}{c^{1/2}} \qquad (9)$$

Assuming that the Griffith equation for a penny-shaped crack is appropriate (actually the P_{cr} will be less than that given by the Griffith equation for a penny-shaped crack, since the crack is more like a half-penny crack), this would give an upper limit to P_{cr} and the resultant overestimate of i_{cr}. The corresponding P_{cr} is given by [11]

$$P_{cr} = \left(\frac{\pi E \gamma_{eff}}{2c(1-\nu^2)}\right)^{1/2} \qquad (10)$$

When P_0 is equal to P_{cr} crack extension will occur. Equating Equations 8 and 10, the critical current density is found to be

$$i_{cr} = \left(\frac{\pi(1-\nu^2)F\gamma_{eff}^2}{8V_m E\eta}\right)\left(\frac{c^2}{l^3}\right) \qquad (11)$$

The primary difference between Equation 11 and previous equations is the incorporation of the crack width $2c$ in a natural way and the resultant different dependency of i_{cr} on l. In the previous two-dimensional calculations, $i_{cr} \propto 1/l$ while the present calculation leads to $i_{cr} \propto 1/l^3$. The magnitude of critical current density for a typical crack may now be evaluated. Taking $\nu = 0.25$, $\eta = 3.4 \times 10^{-3}$ poise (at 300° C), $F = 96\,487$ coulombs mol^{-1},

$V_m = 23.7\,cm^3\,mol^{-1}$, $E = 2.07 \times 10^{12}$ dynes cm^{-2} and $\gamma_{eff} = 5000$ ergs cm^{-2},* we obtain

$$i_{cr} = 16.73 \times 10^4 \left(\frac{c^2}{l^3}\right) \text{amps cm}^{-2} \quad (11a)$$

with c and l in cm.

To compare the results of the present model with the earlier two-dimensional models, crack dimensions have been chosen as before [1–4]. For a crack length 100 μm and width 60 μm, the calculated value of i_{cr} is about 150.6 A cm^{-2}. A similar calculation based on the two-dimensional approaches given previously yields a value of $i_{cr} \simeq 3000$ A cm^{-2}. For a crack of length 200 μm with 60 μm width, the present calculation yields a value of i_{cr} of about 18.8 A cm^{-2} while the two-dimensional approach yields a value of $i_{cr} \simeq 1500$ A cm^{-2}. The value of $2c = 60\,\mu$m chosen is a typical value often observed experimentally. It is important to recognize that although we have chosen the width $2c$ arbitrarily, the corresponding crack opening displacement is automatically built into the analysis. The present calculations clearly demonstrate the profound effect on i_{cr} when the three-dimensional nature of the problem is incorporated into the analysis. With reference to the three-dimensional problem, two important differences are (a) the failure stress does not depend upon crack length but rather on the minor dimension, crack width; and (b) the effect of ion focusing is greater in comparison with the two-dimensional problem (since in the two-dimensional problem, the focusing and the volume flow rate are proportional to $2l$ while in the three-dimensional problem they are proportional to $(\pi l^2/2c)$. Thus, when $l \gg 2c$, the volume flow rate is greater in the three-dimensional case). Both of these effects conspire towards lowering the critical current density.

It should be emphasized that the exact details regarding the geometry of the crack, the dynamic pressure distribution of the fluid flow and the resultant stress distribution in β''-alumina are mathematically complex and beyond the scope of this paper. All that is possible here is to provide an order of magnitude calculation. The approach given here clearly shows that very reasonable values of i_{cr} result from this analysis. Experimental results (in the present investigation) have in fact shown that the i_{cr} at 300° C is somewhere in the range of 10 A cm^{-2} to 20 A cm^{-2}. Furthermore, other aspects such as wetting characteristics and microstructural effects tend to further reduce i_{cr}. Experimental results as well as these other factors are discussed in the following sections.

2.3. Effect of microstructure on degradation

In the analysis presented so far, the crack was assumed to be in the form of a ribbon of width $2c$ and length l. Pressure generated on the crack faces was determined based on the Hagen–Poiseuille law. In reality, the crack will not be flat and smooth (in the x–y plane) as assumed in the analysis, but will be jagged due to the presence of grain boundaries and cleavage planes. Sodium formed at the tip must flow towards the open end through a jagged channel. Consequently, there will be a pressure head loss at every bend. Since the volume flow rate is controlled by the crack length l and the crack width $2c$, and the pressure at the open end is nearly zero, the presence of bends would tend to increase P_0 beyond that given by Equation 8. This should lead to a lowering of the critical current density. Let us assume that l is the length of the crack and $2c$ is the width. The crack consists of n segments, each of dimension D as shown in Fig. 4. Therefore, $l = nD$. However, the extended length of the crack (pipe) is $l_{ext} = l/\cos\theta = nD/\cos\theta$, with the length of each segment being $D/\cos\theta$. Over one segment, the crack opening displacement (b) may be assumed to be constant. The actual pressure distribution will be given by the one calculated previously with the bend losses superimposed at every bend. The two contributions to the pressure drop between y and $y - dy$, namely $dP_{(1)}$ and $dP_{(2)}$, are due to the Poiseuille flow and the head loss at bends, respectively.

Now, $dP_{(1)}$ is given by

$$dP_{(1)} = \left(\frac{\eta V_m E^3}{2(1-\nu^2)^3 F}\right)\left(\frac{l^2 i}{c^4 P^3}\right)\left(\frac{dy}{\cos\theta}\right) \quad (12)$$

which is the same as Equation 6 except for the multiplication factor $1/\cos\theta$.

In order to estimate $dP_{(2)}$, let us assume that there are n bends in the crack. Thus, the number

*On hotpressed β''-alumina, Virkar and Gordon [13] gave $\gamma_{eff} \simeq 15$ to 20 J m^{-2}. However, subsequent work on sintered samples yielded $\gamma_{eff} \simeq 5$ J m^{-2}.

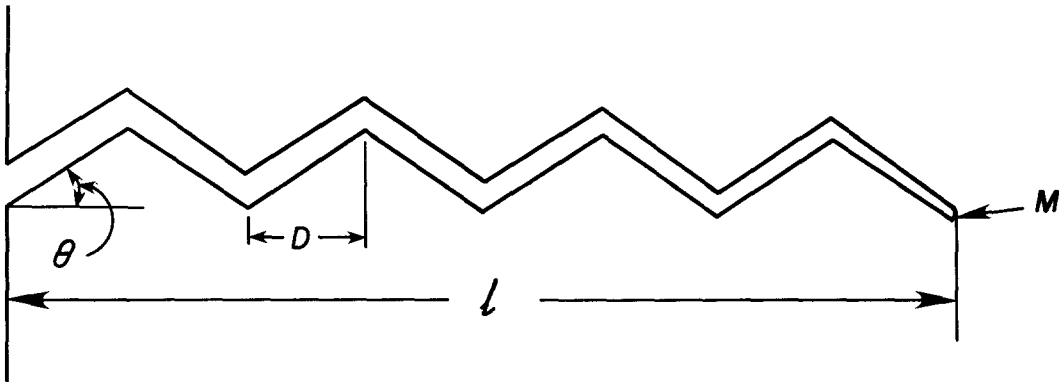

Figure 4 A schematic showing the tortuous nature of a crack in a solid electrolyte.

of bends in length dy is given by $n\,\mathrm{d}y/l$. The pressure drop at a bend is given by [14]

$$P_B = \left(\frac{K\rho}{2}\right)\left(\frac{\dot{V}}{\text{area}}\right)^2 \tag{13}$$

where K is a constant depending upon the bend characteristics (e.g. angle), $\dot{V}$ is the volume flow rate, ρ is the density of the fluid, and area is the cross-sectional area. Substituting for $\dot{V}$ and area ($=\pi bc$),

$$P_B = \frac{K\rho V_m^2 E^2 l^4 i^2}{8F^2(1-\nu^2)^2 c^4 P^2} \tag{14}$$

Since there are $n\,\mathrm{d}y/l$ bends in dy

$$\mathrm{d}P_{(2)} = \frac{K\rho V_m^2 E^2 l^3 i^2 n\,\mathrm{d}y}{8F^2(1-\nu^2)^2 c^4 P^2} \tag{15}$$

The net pressure drop between y and $y-\mathrm{d}y$ is

$$\mathrm{d}P = \mathrm{d}P_{(1)} + \mathrm{d}P_{(2)} \tag{16}$$

Equation 16 can be easily integrated to yield

$$l = \frac{P_0^3}{3B} + \frac{A^2 P_0}{B^3} - \frac{AP_0^2}{2B^2} - \frac{A^3}{B^4}\left[\ln\left(1+\frac{B}{A}P_0\right)\right] \tag{17}$$

where

$$A = \frac{\eta V_m E^3 l^2 i}{2(1-\nu^2)^3 F c^4 \cos\theta}$$

and

$$B = \frac{K\rho V_m^2 E^2 l^3 n i^2}{8F^2(1-\nu^2)^2 c^4}$$

For a given crack width $2c$, the critical pressure, P_{cr}, can be evaluated using Equation 10. This value is substituted for P_0 in Equation 17 and the corresponding current density i, which is the critical current density, can be evaluated numerically.

A considerable simplification of Equation 17 is realized by noting that $\{-A^3/B^4[\ln(1+(B/A)P_0)]\}$ can be expanded as

$$-\left(\frac{A^3}{B^4}\right)\ln\left(1+\frac{B}{A}P_0\right) = -\left(\frac{A^2}{B^3}\right)P_0 + \left(\frac{A}{2B^2}\right)P_0^2 - \left(\frac{P_0^3}{3B}\right) + \left(\frac{P_0^4}{4A}\right) - \left(\frac{B}{5A^2}\right)P_0^5 + \ldots \tag{18}$$

and that the first three terms of this expression cancel out with the first three terms of Equation 17. Furthermore, in the expansion of Equation 18 only the first five terms need be considered since for any reasonable current density, $(B/A)P_0 \ll 1$. It is easily shown that

$$i_{cr} = \left(\frac{\pi^2(1-\nu^2)F\gamma_{eff}^2 c^2\cos\theta}{8V_m E\eta l^3}\right)\left(1 - \frac{K\rho n(1-\nu^2)^4 P_{cr}^5 c^4 \cos^2\theta}{10\eta^2 E^4 l^2}\right)$$

or

$$i_{cr} = i_{cr(0)}\cos\theta - i_{cr(0)}\cos^3\theta \times \frac{K\rho n(1-\nu^2)^4 P_{cr}^5 c^4}{10\eta^2 E^4 l^2} \tag{19}$$

where $i_{cr(0)}$ is the critical current density for a straight crack. Equation 19 shows that there are two factors which tend to reduce the critical current density. The jagged nature of the crack implies effectively longer crack length; this effect being introduced in the first term via $\cos\theta$. The other effect is the head loss at bends which is the second term in Equation 19. Numerical calcu-

lations indicate that the second term is considerably smaller than the first term for reasonable values of n and K. For example, if $n = 10^4\,\text{cm}^{-1}$, i.e. one bend per micrometre, the second term is three orders of magnitude smaller than the first term. Therefore, it is concluded that the grain size will have little effect on i_{cr}. However, with increasing grain size, it is to be expected that c will increase. Thus, there could be in fact an increase in i_{cr} with increasing grain size. This is of some significance since often the objective of a processor is to fabricate fine grained ceramic. With reference to solid electrolytes such as β''-alumina, fine grained microstructure may not be necessary; and in fact a somewhat coarser microstructure may be desirable.

The tortuosity of the crack, however, does affect the critical current density through the term of $\cos\theta$. For example, if $\theta = 45°$, the critical current density for a crack length 200 μm and width ($2c$) 60 μm, is $12.2\,\text{A cm}^{-2}$ instead of $18.8\,\text{A cm}^{-2}$ for a straight crack.

3. Experimental procedure and results

Bar shaped specimens of β''-alumina were sintered to near theoretical density (> 98%) by the procedure described previously [15]. A small hole of about 1.5 mm diameter was drilled along the length of the specimen to a depth of about 1 cm. An α-alumina tube was sealed to each specimen as shown in Fig. 5. A fine copper wire was introduced through the alumina tube such that the tip of the wire was in electrical contact with β''-alumina at the bottom of the hole. A vacuum torr fitting was attached to the other end of the α-alumina tube to which a copper tube was connected. The copper tube was subsequently evacuated. The bottom end of the β''-alumina specimen was dipped in molten $NaNO_3 + NaNO_2$ eutectic at 300° C. The samples were then electrolysed using a d.c. power supply (see Fig. 5). Initially, the current density was kept very low. The α-alumina tube with the copper wire as an electrode was seen to fill with sodium. Slowly the current was increased in increments of 5 mA. After 5 min intervals it was increased in increments of 10 mA. Above a certain current for a given specimen, sodium filament could be seen to initiate from the bottom of the hole and grow. The corresponding current density was determined based on the diameter (area) of the hole. Several such experiments were conducted. The current density above which degradation was observed was between 10 and $20\,\text{A cm}^{-2}$ which is quite consistent with the theoretical calculations presented here. After the experiment the samples were ground to observe the crack in different sections. One such section is shown in Fig. 6. The crack is filled with sodium, which reacts with atmosphere on exposure. It should be noted that this crack is not in its initial stages of propagation. It is difficult to locate the critical crack before it propagates. However, the photomicrograph does indicate that the assumption of a ribbon shaped crack has a sound basis. Furthermore, experimental observation clearly shows that the filament grows in length

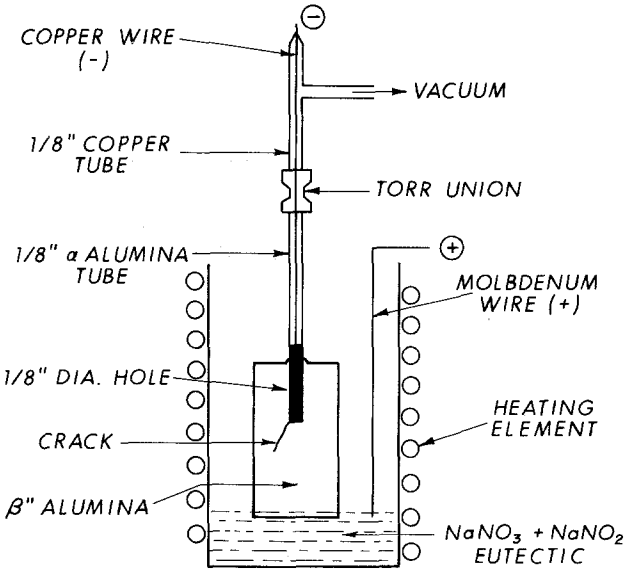

Figure 5 Experimental apparatus used for determining i_{cr} in β''-alumina at 300° C.

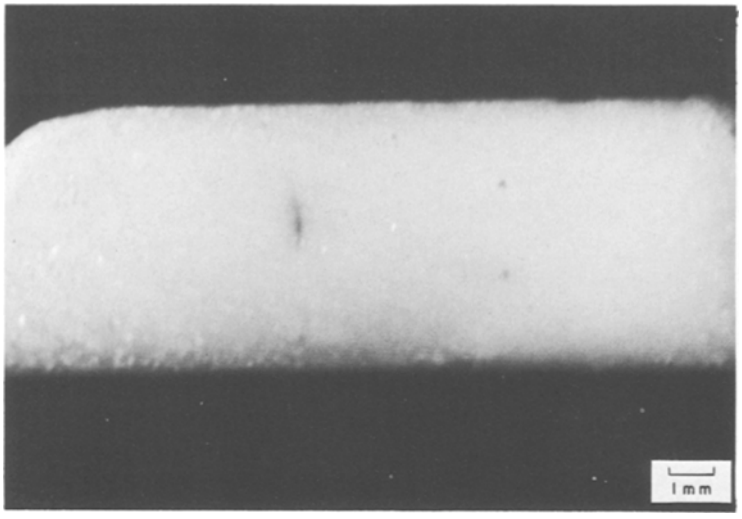

Figure 6 Photograph of β''-alumina surface which was cut perpendicular to the direction of filament growth. A section of the sodium filled filament can be seen.

with little increment in width. Thus, the assumption of $2c$ nearly constant appears reasonable.*

4. Discussion

Semiquantitative but three-dimensional analysis of the solid electrolyte degradation problem presented here clearly demonstrates the essential features of the filament propagation. The critical current densities that result from the analysis given here are entirely consistent with experimental observations. While an exact analysis of the three-dimensional problem is mathematically complex, the present analysis provides some insight into the physical aspects of the degradation process. Although the analyses presented by Shetty *et al.* [4], Feldman and DeJonghe [6] and Virkar [7] are essentially correct within the formalism of the two-dimensional problem, these analyses do not adequately describe the actual degradation process. This is clearly evidenced by the fact that extremely high values of critical current density result out of these analyses which are not in accord with experimental observations. On the other hand, the filament geometry assumed in the present analysis as well as the resulting i_{cr} values are in good agreement with experimental observations.

In the analysis presented here, when the pressure at the tip reaches critical pressure based on a penny-shaped crack of diameter $2c$, the crack is assumed to extend along the length of the crack (along y, Fig. 1a). However, the stress required for the extension of a crack of dimension $2c$ based on a plane strain Griffith equation is in fact less than that for a penny-shaped crack. This would imply that the crack will grow in the x-direction as well near the tip. The implication, therefore, is that as the crack extends in the y-direction, it also extends in the x-direction. However, as the crack extends in the x-direction, the cross-sectional area (in the xz plane, Fig. 1a) increases leading to the lowering of pressure. Consequently, it should not extend much in the x-direction. Furthermore, the magnitude of the pressure at the tip of the crack (point M in Fig. 1a) would be considerably greater than P_0 calculated here for the reasons discussed earlier. Although the details of the crack extension process are difficult to evaluate it is gratifying to note the experimental observations that the filaments almost always grow along the length with very little widening in the x-direction (Fig. 1a).

The effect of nonwetted regions or the regions of large charge transfer resistance can now be assessed in light of the present analysis. Specifically, it was shown by Virkar *et al.* [16, 17] that current density near nonwetted regions can be considerably higher than the applied current density. In reference [16], supporting experimental evidence was provided. Current intensification by a factor of two to three can be easily realized in such regions. It has been argued [6] however that once a crack in such a region grows to some length, it no longer experiences a high enough current density and therefore should arrest. This

*The present analysis will be applicable even if $2c$ is not constant, as long as the rate of growth of $2c$ is much less than the rate of growth of l.

conclusion could perhaps be justified on the basis of the two-dimensional model in which i_{cr} was found to be proportional to l^{-1}. However, the present analysis shows that $i_{cr} \propto l^{-3}$. Thus, even if the crack grows out of regions of locally high current densities, as the critical current density rapidly drops with increasing l, continued propagation is to be expected and the crack should not arrest. This is in accord with the experimental observations. Other evidence of the effect of nonwetting is obtained from the work of Richman and Tennenhouse [2] who observed a critical current density of the order of 1 to 1.5 $A\,cm^{-2}$ when mercury was used as a cathode (subsequently we have obtained similar results using mercury as a cathode). However, when sodium is used as a cathode, current densities in excess of 5 $A\,cm^{-2}$ can be passed without any signs of degradation. The main distinction between these two sets of experiments is that mercury, which was used as a cathode, does not wet β''-alumina properly and exhibits a very high charge transfer resistance. Recent calculations of Wright *et al.* [18] who used the conformal method of Papamichael and Whiteman [19, 20] to evaluate current concentrations near nonwetted regions in electrolytes of finite thickness show that nonwetted regions on the surface of solid electrolyte have a rather large effect.

Some researchers [21] have used acoustic emission methods to determine critical current densities and have obtained acoustic signals at rather low current densities (several $mA\,cm^{-2}$) and therefore have interpreted that the degradation process must have ensued. However, no evidence was presented to indicate that degradation had actually begun. Ample evidence is available which shows that current densities in excess of 1 to 2 $A\,cm^{-2}$ can be passed for prolonged periods of time without failure suggesting that i_{cr} is at least greater than 1 to 2 $A\,cm^{-2}$. The utility of the acoustic emission method to detect the initiation of the degradation process is therefore questionable. Some authors have claimed that degradation of β''-alumina may occur by the precipitation of sodium metal at the operating temperature due to either electron injection [22] or gradient in transference number [23]. Presumably, the sodium deposited develops sufficient pressure to cause ultimate failure of the electrolyte. However, no experimental evidence has been provided which shows occurrence of failure by this mechanism (the so-called mode II). Furthermore, these authors have failed to recognize that if a sodium filled pore leads to a crack formation, the crack will invariably extend in one direction, not both. In that case, if the crack opens up on the sodium side, further extension will have to occur by the Poiseuille pressure model as described in this paper. A crack opening up on the sulphur side should remain benign. Thus, in light of the above reasons, it is unlikely that the so-called mode II would lead to electrolyte failure even though sodium precipitation may be observed.

5. Conclusions

The three-dimensional analysis presented here leads to critical current densities which are in accord with experimental observations. The degradation of solid electrolytes, and in particular that of β- and β''-alumina, under electrolytic conditions can be adequately described by the Poiseuille pressure model in a natural way.

Acknowledgements

This research was supported by the US Department of Energy under Contract No. DE-AS02-77ER04451.

References

1. R. D. ARMSTRONG, T. DICKINSON and J. TURNER, *Electrochim. Acta* **19** (1974) 187.
2. R. H. RICHMAN and G. J. TENNENHOUSE, *J. Amer. Ceram. Soc.* **58** (1975) 63.
3. G. J. TENNENHOUSE, R. C. KU, R. H. RICHMAN and T. J. WHALEN, *Bull. Amer. Ceram. Soc.* **54** (1975) 523.
4. D. K. SHETTY, A. V. VIRKAR and R. S. GORDON, in "Fracture Mechanics of Ceramics" Vol. 4, edited by R. C. Bradt, D. P. H. Hasselman and F. F. Lange (Plenum Press, New York, 1978) p. 651.
5. I. M. SNEDDON and S. C. DAS, *Int. J. Eng. Sci.* 9 (1971) 25.
6. L. A. FELDMAN and L. C. DEJONGHE, *J. Mater. Sci.* **17** (1982) 517.
7. A. V. VIRKAR, *ibid.* **16** (1981) 1142.
8. S. P. TIMOSHENKO and J. M. GODDIER, "Theory of Elasticity" 3rd edn (McGraw-Hill Book Company, New York, 1970) p. 39.
9. P. M. RANDALL, *Amer. Soc. Test. Mater., Spec. Tech. Publ. No.* **410** (1967) 83.
10. G. K. BANSAL, *J. Amer. Ceram. Soc.* **59** (1976) 87.
11. I. N. SNEDDON and M. LOWENGRUB, "Crack Problems in the Classical Theory of Elasticity" (John Wiley and Sons, New York, 1969).
12. R. BERKER, in "Handbuck der Physik" Vol. 802, edited by S. Fluegge (Springer-Verlag, Berlin, 1963) p. 69.

13. A. V. VIRKAR and R. S. GORDON, *J. Amer. Ceram. Soc.* **60** (1977) 58.
14. V. L. STREETER, "Handbook of Fluid Dynamics" (McGraw-Hill, New York, 1961) pp. 3–22.
15. G. YOUNGBLOOD, A. V. VIRKAR, W. R. CANNON and R. S. GORDON, *Bull. Amer. Ceram. Soc.* **56** (1977) 206.
16. A. V. VIRKAR, L. VISWANATHAN and D. R. BISWAS, *J. Mater. Sci.* **15** (1980) 302.
17. A. V. VIRKAR and G. R. MILLER, "Fast Ion Transport in Solids", edited by P. Vashishta, J. N. Mundy and G. K. Shenoy (North Holland Press, New York, 1979) p. 87.
18. A. WRIGHT, L. VISWANATHAN and A. V. VIRKAR, *J. Electrochem. Soc.* in press.
19. J. R. WHITEMAN and N. PAPAMICHAEL, *J. Appl. Math. Phys. (ZAMP)* **23** (1972) 655.
20. N. PAPAMICHAEL and J. R. WHITEMAN, *ibid.* **24** (1973) 304.
21. L. DEJONGHE, presented at the American Ceramic Society Conference in Washington DC, May 1981.
22. L. DEJONGHE, L. FELDMAN and A. BEUCHELE, *J. Mater. Sci.* **16** (1981) 780.
23. L. DEJONGHE, *J. Electrochem. Soc.* **129** (1982) 752.

Received 30 April
and accepted 13 September 1982